Published in final edited form as:
Cell Rep. 2014 June 26; 7(6): 1926–1939. doi:10.1016/j.celrep.2014.05.021.

Age-related dysfunction in mechano-transduction impairs differentiation of human mammary epithelial progenitors

Fanny A. Pelissier[1,2], **James C. Garbe**[1], **Badriprasad Ananthanarayanan**[4], **Masaru Miyano**[1], **ChunHan Lin**[1,3], **Tiina Jokela**[1,2], **Sanjay Kumar**[4], **Martha R. Stampfer**[1], **James B. Lorens**[2], and **Mark A. LaBarge**[1,*]

[1]Life Science Division, Lawrence Berkeley National Laboratory, Berkeley, CA 94720, USA

[2]Center for Cancer Biomarkers, Department of Biomedicine, University of Bergen, Bergen N-5009, Norway

[3]Department of Comparative Biochemistry, University of California, Berkeley, CA 94720, USA

[4]Department of Bioengineering, University of California, Berkeley, CA 94720, USA

Summary

Dysfunctional progenitor and luminal cells with acquired basal cell properties accumulate during human mammary epithelia aging for reasons not understood. Multipotent progenitors from women aged <30 years were exposed to a physiologically relevant range of matrix elastic modulus, and increased rigidity caused a differentiation bias towards myoepithelial cells while reducing production of luminal cells and progenitor maintenance. Lineage representation in progenitors from women >55 years was unaffected by physiological modulus changes. Efficient activation of Hippo pathway transducers YAP and TAZ was required for the modulus-dependent myoepithelial/basal-bias in younger progenitors. In older progenitors YAP/TAZ were only activated when stressed by extra-physiologically rigid matrices, which biased differentiation towards luminal-like phenotypes. YAP was primarily active in myoepithelia of younger breast tissues, but activity increased in luminal cells with age. Thus aging phenotypes of mammary epithelia may arise partly because alterations in Hippo pathway activation affect the processes of progenitor differentiation and lineage specificity.

*Correspondence, MALabarge@lbl.gov, 1 Cyclotron Road; MS977; Berkeley, CA 94720 USA, Phone: 510-486-4544; FAX: 510-486-5568.

Author contributions

FP, JBL, and MAL designed the research; FP, JCG, BA, MM, CHL, TJ, and MAL performed experiments; JCG, MRS, SK, and MAL provided cell strains and other key reagents; FP, MRS, JBL, and MAL wrote the manuscript.

Introduction

The aging process is often correlated with changes in stem cell activity with consequences ranging from reduced regenerative capacity to increased cancer incidence. Human hematopoietic stem cells accumulate with age(Kuranda et al., 2011; Pang et al., 2011) and exhibit a differentiation bias towards defective myeloid lineages(Cho et al., 2008), making individuals more prone to auto-immune problems and myeloid leukemias(Henry et al., 2011). In mice, the proportion of mitotic neural stem cells increases with age, whereas numbers of adult-born neurons decrease(Stoll et al., 2011). Human hippocampus shows patterns of age-related changes similar to mice that may underlie age-related cognitive decline(Knoth et al., 2010). Transit amplifying cells, not stem cells, accumulate in epidermis with age and delay wound healing(Charruyer et al., 2009). Mammary epithelium is maintained by a hierarchy of lineage-biased and multipotent progenitor and stem cells (Nguyen et al., 2014; Rios et al., 2014; Villadsen et al., 2007). In human mammary gland, differentiation-defective cKit-expressing multipotent progenitors (MPP) accumulate with age, and proportions of daughter myoepithelial (MEP) and luminal epithelial (LEP) cells shift with age. We hypothesized that these age-associated changes make aged breast tissue susceptible to malignant progression(Garbe et al., 2012). Accumulation of defective stem or progenitor cells may be a common phenotype among aging tissues, and we hypothesize that aged MPP accumulate because they do not correctly perceive microenvironmental differentiation cues.

The molecular composition of microenvironments impose specific cell fate decisions in normal and immortal non-malignant mammary MPP(LaBarge et al., 2009). Cell culture substrata tuned to elastic moduli that mimicked normal breast tissue also biased the differentiation of an immortal non-malignant MPP cell line into LEP(Lui et al., 2011). Matrix stiffness is mechanistically important in breast cancer progression as well; rigid breast tissue correlates with high breast cancer risk and drives malignant phenotypes in breast cancer cell lines(Yu et al., 2011). The physiological range of elastic modulus in breast likely plays an instructive role in the differentiation of normal mammary epithelial progenitors.

Membrane and cytoskeleton proteins sense mechanical cues and trigger transduction cascades that relay information throughout the cytoskeleton and to the nucleus. Responses can include changes in morphology and gene expression(Vogel and Sheetz, 2006). Sensing matrix elasticity occurs through cell-cell and cell-ECM interactions mediated by adherens, integrins, vinculin, focal adhesion kinase (FAK) and others(Beningo et al., 2001; Bershadsky et al., 2003; Tamada et al., 2004). The actinomyosin network includes RhoA, which regulates the actin cytoskeleton in the formation of stress fibers (SF) and focal adhesions (FA). Activation of ROCK1/2 causes increased activity of the motor protein myosin II by phosphorylation of the myosin light chain (MLC) and inactivation of the MLC phosphatase(Ishizaki et al., 1997; Kimura et al., 1996). YAP and TAZ are Hippo pathway transcriptional co-activators that are thought to interact with the Rho pathway to transduce mechanical from the microenvironment to the nucleus(Halder et al., 2012). As stiffness increases YAP/TAZ relocates from cytoplasm into nucleus, where they generate gene expression patterns that underlie cellular functions like proliferation, migration, epithelial to

mesenchymal transition, and differentiation(Dupont et al., 2011; Kanai et al., 2000; Zhao et al., 2007).

Differentiation of mesenchymal stem cells down neurogenic, myogenic, or osteogenic pathways was directed by exposure to a wide range of tissue-relevant elastic moduli, from 100Pa~40,000Pa(Engler et al., 2006). Mammary MPP differentiation should be responsive to a much narrower range of modulus relevant to normal and malignant breast (100Pa ~4000Pa)(Paszek et al., 2005). The impact of aging on modulus-directed differentiation is unknown. Addressing these issues required a culture-based platform for functional analyses of primary normal human mammary MPP from many individuals. Here we used such an approach to demonstrate that differentiation patterns of MPP from women aged <30 (y)ears cultured on tunable 2-D and 3-D substrata were exquisitely responsive to a physiologically relevant range of elastic modulus in a YAP/TAZ dependent manner. Whereas MPP from women >55y were relatively unresponsive to changes in rigidity due to inefficient activation of the Hippo pathway transducers.

Results

Aging alters modulus-dependent differentiation

To test whether microenvironment rigidity directed differentiation in MPP, we enriched receptor tyrosine kinase cKit-expressing (cKit+) human mammary epithelial cells (HMEC) by flow cytometry (FACS) from 4th passage primary pre-stasis HMEC (strains) derived from 5 women aged <30y and 5 from women >55y (Fig S1, Table S1). Pre-stasis HMEC strains are normal and not treated with any immortalizing agents, have finite lifespans, and we previously demonstrated that they retain molecular, biochemical, and functional properties consistent with aging in vivo(Garbe et al., 2012). The cKit+ MPP were cultured for 48h on type 1 collagen-coated polyacrylamide (PA) gels. The Young's elastic modulus (E(Pa)scals) of the PA gels was tuned from 200Pa to 2350Pa. The lineage of each daughter cell was confirmed by immunofluorescence (IF) of intermediate filament proteins keratin (K)14 and K19, CD227 (Sialomucin-1), and CD10 (Calla) (Fig 1A,B,E,F). Computer image analysis identified the different lineages; LEP are $CD227^{+}/CD10^{-}/K14^{-}/K19^{+}$, MEP are $CD227^{-}/CD10^{+}/K14^{+}/K19^{-}$, and $K14^{+}K19^{+}$ expression is consistent with MPP states (Villadsen et al., 2007). cKit+ MPP from women <30y generated proportionately more LEP on soft substrata, but generation of MEP increased with higher E (Fig 1C, C', G and S2A). cKit+ MPP from women >55y did not generate different lineage proportions in response to changes in E (Fig 1D, D', H and S2B). Primary 1st passage cKit+ MPP, from 3 women <30y, embedded in tunable 3-D hydrogels with some type 1 collagen for 7 days (Fig S3A) (Ananthanarayanan et al., 2011), gave rise to more LEP at 120Pa versus more MEP at 3800Pa (Fig 1K, M, M' and S3B). In contrast, cKit+ MPP from 3 women >55y did not display modulus-dependent differentiation patterns (Fig 1L, N, N' and S3C). The proportion of K14+/K19+ MPP decreased with elastic modulus on 2-D PA gels and in 3-D gels <30y HMEC (Fig S4A–C), but no change in proportions of MPP was observed >55y HMEC (Fig S4B, D and F). These results suggested that differentiation was modulus-dependent in younger MPP, and that this response was lost with age.

To test if changes in lineage proportions were due to lineage-biased proliferation, incorporation of 5-ethynyl-2'-deoxyuridine (EdU) into DNA was measured as a proxy for proliferation. All lineages derived after 48h from cKit+ MPP on PA gels exhibited similar proportions of EdU incorporation (EdU^+) irrespective of substrate rigidity or age (Fig 1I). In contrast, EdU incorporation in unsorted HMEC strains, which are primarily composed of more mature LEP and MEP, revealed age- and lineage-specific replicative behaviors. Proportions of EdU^+ MEP from <30y HMEC significantly increased with greater E while EdU^+ LEP trended downward (Fig 1J). Unsorted HMEC from women >55y exhibited neither lineage- nor modulus-dependent proliferation (Fig 1J), underscoring the lack of mechano-response with age. Thus changes in lineage proportions exhibited by <30y MPP after 48h were likely due to modulus-dependent differentiation, and only after the lineages matured in <30y HMEC strains did they show evidence of modulus-dependent proliferation.

Mechano-sensing functions were unaltered by age

To determine whether mechano-sensing was age-dependent, F-actin SF formation and FA assembly activities were measured in cKit+ MPP from 3 <30y and 3 >55y strains. Irrespective of age, SF formation increased with greater E (Fig 2A). Homogeneity measurements were used to quantify formation of the F-actin cables (Haralick et al., 1973; Pantic et al., 2012), SF homogeneity was inversely proportional to E in both age groups, which showed similar slopes (Fig 2B,C). Progenitors from both age groups were stained for pFAK and vinculin, which co-localize at FA. More FA assemblies were observed with increased E at the MPP-gel interfaces, and FA formation was not impaired with age (Fig 2D,E). FA homogeneity was inversely proportional to E with comparable slopes in both age groups (Fig 2F,G). Thus, similar SF and FA phenotypes were observed both in younger and older cKit+ MPP.

Extracellular signal regulated kinase (ERK) is phosphorylated in response to increased elastic modulus in some adherent cell lines (Provenzano et al., 2009) and because it is a key effector of serum responses, changes in its modulation could cause pleiotropic cellular responses. Both young and old cKit+ MPP exhibited a low level of ERK phosphorylation on 200Pa PA gels, but increased up to 15-fold on 2350Pa PA gels (Fig 2H,I). Differences in pERK were not significant between age groups, and MAPK inhibitor PD98059 prevented ERK phosphorylation in all cases. By these measures, modulus-dependent activity in serum response was independent of age.

If mechano-sensing was unaffected by aging, then perturbations of actinomyosin regulators that are known to alter FA or SF formation should elicit parallel phenotypes in young and old MPP. Independent of age, we observed that inhibitors of ROCK1/2 (Y27632), and MLC kinase (MLCK) (ML-7) tended to disrupt SF on 2350Pa substrata and showed little effect at 200Pa, whereas the MLC phosphatase (MLCP) inhibitor calyculin A (calA) caused SF formation at 200Pa (Fig 3A,B). Patterns of changes in F-actin homogeneity were parallel in both age groups (Fig 3C,D). Y27632 and ML-7 disrupted the FA assemblies on 2350Pa substrata, whereas calA promoted FA assembly on 200Pa substrata (Fig 3E,F) and measurements of FA homogeneity showed parallel changes in both age groups (Fig 3G,H). Mechano-sensing of substrata in the physiologically relevant range was age-independent,

evaluated by these measures, and thus was unlikely to account for age-dependent differences in mechanically-directed differentiation.

Analysis of the effects of actinomyosin network modulation on differentiation in 3 young and 3 old cKit+ MPP revealed surprising age-dependent responses. FA and SF in cells treated with Y27632 and ML-7 on 2350Pa gels were similar to untreated cells on 200Pa gels, whereas calA increased the SF and FA as if cells were on stiffer substrata. Thus, SF and FA phenotypes were pharmacologically manipulated irrespective of the actual substrate E. Younger cKit+ MPP treated with Y27632 or ML-7 significantly increased proportions of K19+ LEP compared to DMSO-treated cells on 2350Pa gels. In contrast, older MPP were unaffected by Y27632 or ML-7 treatment (Fig S5). Interestingly, CalA increased MEP generation from young MPP, but caused older MPP to give rise to significantly more LEP. No changes in proportion were observed on 200Pa gels suggesting that addition of CalA was insufficient to trigger cell differentiation on such a soft substrata. Older progenitors did not respond to chemically decreased perception of stiffness, but they responded to artificially higher stiffness oppositely to that of young progenitors, suggesting that age-dependent transcriptional programs were operative.

Aging alters the ability of YAP and TAZ to transduce mechanical information to the nucleus

We next determined whether the mechano-transducive transcription factors YAP and TAZ were involved in modulus-dependent differentiation. IF staining of YAP and TAZ in cKit+ MPP from 3 HMEC strains <30y exhibited increased YAP/TAZ nuclear translocation as PA gel E increased from 200 to 2350Pa (Fig 4A,B). However, significant nuclear translocation of YAP/TAZ was not observed in older progenitors in the same range (Fig 4C,D). The ability to activate YAP/TAZ by changes in substrate E was age-dependent.

To determine the extent to which YAP/TAZ was unresponsive to changes in E in older progenitors, we evaluated their activation in response to extra-physiological stiffness. cKit+ MPP from 3 young and 3 old strains were cultured on type 1 collagen-coated glass (>3GigaPa) or 200Pa gels. YAP/TAZ translocated to the nucleus in young cKit+ MPP on glass (Fig 4A,B), gave rise to fewer LEP (Fig 4E) and those LEP incorporated less EdU on glass compared to 200Pa gels (Fig 4F). In older cKit+ MPP on glass, YAP/TAZ was nuclear (Fig 4C,D), but cells gave rise to more LEP (Fig 4G), which incorporated more EdU on glass than on 200Pa gels (Fig 4H). Both calA treatment and culture on extra-physiologically rigid substrata elicited more LEP differentiation in older MPP, which was strikingly the opposite of younger MPP. Thus the Hippo-pathway mechano-response in older progenitors was shifted to an extra-physiological ‘trigger point’.

To determine if YAP and TAZ were required for modulus-dependent differentiation, both in the physiological and extra-physiological ranges, cKit+ MPP were transfected with siRNAs, siYAP or siTAZ, which achieved >70% knockdown of the respective mRNAs (Fig 4K). K14 and K19 proteins were measured by IF in each cell after 48 hours on PA gels. Younger MPP harboring either siYAP or siTAZ were unable to give rise to more MEP on 2350Pa PA gels and glass substrata compared to controls (Fig 4I). In older MPP, siYAP and siTAZ had no effect at 200Pa or 2350Pa, but they prevented the generation of more LEP on glass (Fig

4J). Thus YAP and TAZ were required for modulus-dependent differentiation in progenitors irrespective of age.

YAP localization changes with age *in vivo*

That YAP and TAZ activity correlated with a bias towards MEP in younger women, prompted us to evaluate normal breast tissue sections from reduction mammoplasty. K14, K19 and YAP were evaluated by IF in sections from four women aged from 34y, 40y, 50y, and 54y (Fig 5A). Multiple fields from each section were analyzed to account for heterogeneity, and marker-based watershed cell segmentation identified levels of YAP in nuclear and cytoplasmic domains of MEP, LEP, and K14+/K19+ putative MPP. YAP staining was localized mainly to the nuclei of MEP and MPP in the 34y and 40y glands. (Fig 5B). In the 34y gland we also observed a few occurrences of K14+/K19- cells that we assumed were LEP based on their luminal location. Upon measuring the YAP signal intensity it was determined that the K14+ cells always correlated with higher YAP expression (Fig 5C). In contrast to younger epithelia, the 50y and 54y glands exhibited no inequality in YAP localization between the different lineages (Fig 5B), and qualitatively the even-appearing distribution of YAP in the nuclei and cytoplasm of the LEP and MEP in older women was reminiscent of YAP staining in >55y HMEC (Fig 5C). YAP distribution in vivo was age-dependent consistent with our findings in primary cultures. Overall, the data suggest that YAP activity is associated with MEP/basal phenotypes, even in the case of LEP in older women that acquire some traits of MEP. That impression was strengthened by our analysis of breast cancer data from The Cancer Genome Atlas data (Cancer Genome Atlas, 2012), which showed that YAP/TAZ mRNA expression negatively correlated with levels of LEP-related proteins and mRNAs, and positively correlated with markers of MEP and with YAP/TAZ target genes (Fig S6A and S6B).

Levels of Hippo pathway components changed with age

To better understand why the ‘trigger point’ for YAP/TAZ was increased in older MPP we determined whether Hippo pathway components showed age-dependent expression patterns. Mst1/2, Lats2, and Angiomotins (AMOT), phosphorylate and sequester YAP/TAZ in the cytoplasm, which would prevent YAP/TAZ from associating with DNA-binding co-factors TEAD1–4 and transcribing target genes, like connective tissue growth factor (CTGF) (Zhao et al., 2007) (Zhao et al., 2011). Analysis with qRT-PCR revealed that in almost all cases *MST1/2*, *LATS2*, *AMOT*, *AMOTL1*, *TEAD1–4*, and *CTGF* were significantly correlated between women <30y and women >55y on 200Pa (Fig 6A, p=0.0110, R=0.7283) and 2350Pa (Fig 6B, p=0.0083, R=0.7464) gels. On glass the correlation was less obvious (Fig 6C, p=0.0543, R= 0.5934). Because differences in hippo gene expression were not strikingly age-dependent in physiological conditions we examined protein levels of MST1 and MST2. MST1 levels from 3 women <30y and 3 women >55y were not significantly different (Fig 6D–G). MST2 protein levels were 3-fold greater in MPP from women >55y compared to <30y on 2350Pa gels (Fig 6E). Thus it is tempting to speculate that age-dependent imbalances of hippo pathway regulators can lead to insensitivity to mechanical cues and activation of YAP/TAZ.

Immortalization restored responsiveness to physiological stiffness

Cellular responses to mechanical stimuli are often examined with mesenchymal stem cells or immortal malignant and non-malignant cell lines. Whereas immortal cell lines tend to proliferate more on stiffer substrata, we showed that normal <30y HMEC exhibited lineage-dependent responses and that <55y HMEC were non-responsive to a physiological range of E (Fig 1). To better understand the differences between the normal and immortal non-malignant states as a function of age, we examined immortal non-malignant cell lines derived from 2 young and 2 old primary HMEC strains by targeted inactivation of senescence barriers combined with unknown genomic errors(Stampfer et al., 2013). The cell lines, 240LMY (19y), 184Fp16s (21y), 122LMY (66y), and 805Pp16s (91y) (Fig S7) were cultured atop PA gels tuned from 200 to 2350Pa. cKit+ MPP from 240LMY and 184Fp16s cell lines gave rise to more K14+ MEP than LEP on glass compared to 200Pa PA gels (Fig 7A). cKit+ MPP from 122LMY and 805Pp16s gave rise to more K19+ LEP than MEP on glass compared to 200Pa PA gels (Fig 7B). Independent of age, all lineages of the immortal cell lines incorporated more EdU as rigidity increased (Fig 7C–F). YAP/TAZ nuclear translocation was detected both in <30y and >55y cell lines on PA gels from 200Pa to 2350Pa (Fig 7G–N). Thus immortalization of older HMEC restored sensitivity of the Hippo pathway to the physiological stiffness range, albeit abnormally because proliferation was no longer lineage dependent. The propensity of immortal cell lines to generate more MEP or LEP on extra-physiological substrata was consistent with the chronological age of the HMEC, suggesting that the intrinsic age-related changes were stable.

Discussion

Matrix rigidity is a determinant of mammary epithelial progenitor differentiation. Exposure of progenitors to mechanically tuned culture substrata revealed two fundamental changes that arise in MPP with age; (i) the mechanical ‘trigger point’ for activation of YAP/TAZ increases, and (ii) the YAP/TAZ-dependent differentiation programs become distinct. Culture of MPP from <30y women in the most compliant 2-D or 3-D conditions (100–200Pa) enhanced LEP differentiation, whereas stiffer substrata (2300–3800Pa) favored MEP production. Older progenitors stochastically differentiated when exposed to a physiologically relevant elastic modulus range. Our results document the role of YAP/TAZ transcription factors as drivers of modulus-dependent differentiation in human mammary epithelial MPP, and suggest that YAP/TAZ activity favors MEP, and other basal cell types, differentiation. The basal cell types are not exclusive to MEP, and may include LEP that express K14 or other basal-associated markers, which we and others have observed(Santagata et al., 2014). Older MPP needed to be stressed with extra-physiologically stiff substrata to reveal their YAP/TAZ-dependent bias towards LEP, which was consistent with our observation in vivo that YAP tended to be located in LEP with increased age. In younger women YAP was in the nuclei of K14-expressing MEP, as well as the apical snouts of LEP. We previously demonstrated that post-menopausal LEP tend to express some K14, as well as other markers associated with MEP, and these new data suggest that age-dependent changes in YAP/TAZ activity may underlie that phenotype of aging.

Radiographic density of breast tissue tends to decrease with age(Benz, 2008), but mechanical forces do not exclusively govern YAP/TAZ regulation in vivo. Although our experimental approach took advantage of tuned mechanical perturbations of matrix to functionally probe the HMEC, more broadly these results revealed that aging fundamentally alters Hippo pathway regulation. The role of cell-cell contact in Hippo pathway regulation should be further investigated in the context of chronological age. Both Wnt/beta-catenin and NF2 also are known to regulate YAP/TAZ in vivo(Cockburn et al., 2013; Imajo et al., 2012), and changes to both pathways have been implicated in different age-related cancers(Evans et al., 2005; Seidler et al., 2004). Little is known about whether YAP/TAZ play a role in other phenotypes of aging. Deficiency in *c.elegans* yap-1 resulted in overall healthier aging relative to controls(Iwasa et al., 2013). Disrupted Hippo signaling in human and mouse ovarian follicles, which caused YAP activation, promoted growth and oocyte maturation, which are processes typically defective with age(Kawamura et al., 2013). Indirect evidence suggests mesenchymal stem cells also have dampened modulus-dependent differentiation responses with age. Bone is magnitudes stiffer than adipose tissue and the osteogenic potential of mesenchymal stem cells decreases and a bias towards adipogenesis increases with age(Moerman et al., 2004), but the role of Hippo is unclear.

Accumulation of MPP with age may be attributed to inefficient transduction of differentiation cues through the Hippo pathway. At low cell density, decreased Lats2 activity dependent on SF formation causes YAP/TAZ to translocate to the nucleus(Wada et al., 2011), but <30y and >55y MPP formed SF and FA comparably in response to changes in matrix stiffness. Thus, we explored the potential for stoichiometric imbalances in Hippo kinases with age that could dampen activation of YAP/TAZ. In our hands, MST2 protein was higher in >55y MPP, suggestive of a damping mechanism. The Hippo pathway is implicated in differentiation of different progenitors into adipose, breast, muscle, and bone tissues, representing a wide range of elastic modulus, and predicting a marvelously adaptable molecular rheostat. Each of these tissues differs in their matrix composition as well as physical attributes, and there is a reasonable expectation that combinations of ECM and growth factors tune Hippo pathway activity. Further study of microenvironment regulation of the Hippo pathway may reveal components of the activation rheostat and reveal the basis for its age-related dampening.

Changes to the mechanical microenvironment effects multiple cell types in breast. High breast stiffness and density are correlated with increased risk and cancer progression (Yu et al., 2011). Increased stiffness also can induce adipocyte progenitors to differentiate into fibroblasts, which can positively feedback to further increase tissue stiffness (Chandler et al., 2012). MPP from women <30y responded to increasingly rigid matrices by increased production of MEP, which are thought to be tumor suppressive (Gudjonsson et al., 2002; Hu et al., 2008), and proportionately decreased numbers of cells with the MPP phenotype, which are hypothesized to be breast cancer cells-of-origin (Lim et al., 2009), suggestive of a protective mechanism from tumor progression in younger epithelia. However, this putative protective mechanism falters with age, as demonstrated when aged HMEC were essentially unresponsive to physiological changes in matrix modulus.

We speculate that the prevalence of luminal subtype breast cancers in post-menopausal women may be the result of age-acquired epigenetic states. When older MPP were exposed to extra-physiologically stiff substrata, they exhibited LEP-biased differentiation - the exact opposite of the younger progenitors. Age-dependent differentiation patterns were preserved in immortal young and old HMEC, but the mechano-transducive mechanism was notably rejuvenated in older immortal cells enabling them to proliferate increasingly as matrix modulus approached that of a tumor. YAP/TAZ were required for shifting production in favor of MEP in younger, and LEP in older MPP on the stiffer surfaces. We hypothesize that the distinct differentiation responses of younger and older MPP reflect age-dependent epigenetic landscapes. Indeed, normal HMEC exhibit age-dependent gene expression patterns consistent with the concept of age-dependent epigenetic states(Garbe et al., 2012). A precedent was set in hematopoietic stem cells where DNA and histone modifications were shown to correlate with age-related functional phenotypes(Chambers et al., 2007). Stromal feedback loops can result in formation of stiffened regions; if such regions already contained an accumulation of aged progenitor cells carrying errors predisposing them to immortality, they could create an environment that promotes development of age-related luminal subtype breast tumors.

Finally, it is important to be able to empirically examine the cell and molecular consequences of aging in normal human epithelia because most carcinomas are age-related. Wild type mice are typically resistant to cancers and murine models of breast cancer do not completely model the steps of cancer progression in HMEC (Stampfer et al., 2013), and most inbred strains exhibit tumor incidence curves consistent with sporadic tumor genesis, thus mice may not be an optimal model for studying the genesis of age-related breast cancers. Here we present an approach for interrogation of human aging that takes advantage of cultured strains of normal HMEC and engineered microenvironments to perform cell-based molecular and functional studies, which are validated by comparison with breast tissues. Most studies that have drawn conclusions from breast cancer cell lines or mouse studies have used three methods to establish relevance of their results to human in vivo: an experiment with primary HMEC that recapitulates the main findings, examination of tissue sections for in vivo evidence that correlates with the findings, and correlation with large gene/protein expression datasets derived from patient samples. We have followed these three conventions. We find it striking that many of the molecular and biochemical phenotypes of aging persist in our early passage strains in spite of the imperfect microenvironment, which reinforces our impression that age-associated epigenetic changes are stabilizing those phenotypes. However, limitations and challenges are endemic to every experimental system. Early pregnancy has a detectable protective effect against breast cancer, and the balance of epithelial lineages and gene expression patterns in mice and humans are affected by parity (Choudhury et al., 2013). Our current strain collection is not annotated for parity information, and focused studies should be conducted to determine how parity modifies the aging phenotype in breast. There is an impressive level of heterogeneity among human mammary epithelia as was beautifully shown by detailed examinations of luminal lineages (Santagata et al., 2014; Shehata et al., 2012). Our method for establishing primary strains encompasses a significant amount of the total heterogeneity in given surgical specimen, and low stress culture conditions maintains MPP activity in early passages

(Labarge et al., 2013). We also addressed this issue of heterogeneity and potential for inter-individual variation by using strains established from seventeen different women, with any given experiment comparing thousands of independent measurements from groups comprised of three to five strains each. We find repeatedly that the functional, molecular, and biochemical phenotypes often differ between the pre- and postmenopausal age groups, underscoring the importance of chronological age as an experimental variable.

Experimental Procedures

Cell Culture

All cell culture was in M87A medium with cholera toxin (CT) at 0.5 ng/ml, and oxytocin (X) at 0.1 nM (Bachem) (Garbe et al., 2009). Primary HMEC strains were generated and maintained as described (Labarge et al., 2013). Modulus-dependent effects were measured in sub-confluent cultures. Supplemental Table S1 shows the strains used for each experiment.

Reagents

Cells were treated with Y27632 (10μM, Sigma), ML-7 (10μM, Sigma) or calyculin A (2nM, Calbiochem) 2h after adhesion. Cells were treated with PD98059 (50μM, CST) 24h after adhesion. Cells were transfected with YAPsi, WWTR1 (TAZsi), or non-targeting control siRNA SMARTpools (Dharmacon/Thermo) plus a FITC label with DharmaFECT reagent according to manufacturer, 24h prior to FACS enrichment.

Flow Cytometry

Anti-CD227-FITC (BD, clone HMPV, 1:50), anti-CD10-PE (BioLegend, clone HI10a, 1:100), and anti-CD117-APC (BioLegend, clone 104D2, 1:50) were added to cells in media for 25min on ice, washed in PBS and sorted. FACSVantage DIVA (Becton Dickinson).

Polyacrylamide (PA) gels

PA gels were made on circular, 12mm coverslips etched in 0.1M NaOH following an adapted protocol (Tse and Engler, 2010). Sulfo-SANPAH (0.4mM) was activated by UV light, then collagen was added (0.1mg/ml in 50mM HEPES, Sigma). ddH_2O washed gels were placed in polyHema-treated (0.133mL at 12mg/ml in 95% EtOH) 24-well plates. Gel modulus was confirmed with atomic force microscopy.

Immunofluorescence

HMEC were fixed in methanol:acetone (1:1) at −20°C for 15 minutes, blocked with PBS, 5% normal goat serum, 0.1% Triton X-100, and incubated with anti-K14 (1:1000, Covance, polyclonal rabbit) and anti-K19 (1:20, Developmental Studies Hybridoma Bank, clone Troma-III) overnight at 4°C, then visualized with fluorescent secondary antibodies (Invitrogen) incubated for 2 hours at room temperature. EdU was added to culture media 4h prior to fixing cells, and was imaged with Alexa647 click reagents (Invitrogen). Paraformaldehyde (2.5%) was used for fixation for phalloidin (1:50, Invitrogen), anti-pFAK (1:1000, Invitrogen, mAb), anti-vinculin (1:400, Sigma, mAb), anti-YAP (1:100, Santa

Cruz, SC-15407), anti-TAZ (1:200, Cell signaling, polyclonal), Phospho-p44/42 MAPK (Erk1/2) (1:100, CST mAb) and p44/42 MAPK (Erk1/2) (1:100, CST mAb). Paraformaldehyde (1.6%) was used for fixation for anti-CD227 (1:200, Abcam, polyclonal) and anti-CD10 (1:100, BD Biosciences, clone HI10a). Paraffin embedded sections were deparaffinized and antigen retrieved (Vector Labs) and stained with primaries antibodies to K14 (1:1000, Covance, PRB-155P; visualized with A647 Zenon probes from Invitrogen), K19 (1:100, AbCAM, AAH07628) and YAP (1:100, Sanata Cruz, SC-15407). Cells were imaged with LSM710 confocal microscope (Carl Zeiss). Image analyses were conducted using a modified watershed method in Matlab software (Mathworks), see supplemental information for detailed code.

Real-time PCR

Total RNA was purified with Trizol (Invitrogen) followed by RNeasy prep (Qiagen). cDNA was synthesized with SuperScript III RT (Invitrogen). Transcripts levels were measured by quantitative real-time PCR (qRT-PCR) using iTaq SYBR Green Supermix (BioRad) and LightCycler480 (Roche). Primer sequences are in the supplement.

Generation of immortal cell lines

Finite lifespan HMEC from specimens 184, 240L, 122L, and 805P were grown in M87A. Retroviral vectors: The p16 shRNA was in MSCV vector, c-Myc was in pBabe-hygro (BH2) or LXSN vector. Retroviral stocks were generated from supernatants collected in M87A medium. Strains 240L, 122L, and 805P at passage 3 or and 184 at passage 4 were transduced with MSCV-p16sh or MSCV control and selected with puromycin. At the next passage, after puromycin selection, the p16sh transduced cells were transduced with c-Myc pBabe–hygro (c-myc LXSN for 184) and selected with hygromycin. Vector only control pre-stasis cells entered stasis at passage 12–15, whereas the immortalized lines continued to grow.

Western Blot

The following antibodies were used: MST1 Cell Signaling #3682 Rabbit 1:1000, MST2 Cell Signaling #3952 Rabbit 1:1000, beta-actin abcam #8227 Rabbit 1:500, and visualized with Goat anti Rabbit IgG (H + L)-HRP Conjugate #170–6515 1:10’000

TCGA database

All data was obtained from the TCGA breast cancer online portal (https://tcgadata.nci.nih.gov/docs/publications/brca_2012/), (Cancer Genome Atlas, 2012). The following files were used: for microarray gene expression data: “BRCA.exp.547.med.txt”, for reverse-phase protein array (RRPA) expression data: “rppaData-403Samp-171Ab-Trimmed.txt”.

Statistical Analysis

Graphpad Prism 5.0 for PC and Matlab were used for all statistical analysis. Standard linear regression was used. Grouped analyses were performed with Bonferonni’s test for multiple

comparisons. To compare two population distributions Chi-squared and t-tests were performed. Significance was established when: *p<0.05, **p<0.01, ***p<0.001.

Supplementary Material

Refer to Web version on PubMed Central for supplementary material.

Acknowledgments

We thank Prof. Matthias Lutolf, Gurkaran S Buxi, and Thibault Vatter for expert advice. ML is supported by NIH (NIA R00AG033176 and R01AG040081, NCI U54CA143836), and the U.S. Department of Energy (DE-AC02-05CH11231). BA is supported by a postdoctoral fellowship from the California Institute for Regenerative Medicine (TG2-01164).

References

Ananthanarayanan B, Kim Y, Kumar S. Elucidating the mechanobiology of malignant brain tumors using a brain matrix-mimetic hyaluronic acid hydrogel platform. Biomaterials. 2011; 32:7913–7923. [PubMed: 21820737]

Beningo KA, Dembo M, Kaverina I, Small JV, Wang YL. Nascent focal adhesions are responsible for the generation of strong propulsive forces in migrating fibroblasts. The Journal of cell biology. 2001; 153:881–888. [PubMed: 11352946]

Benz CC. Impact of aging on the biology of breast cancer. Critical reviews in oncology/hematology. 2008; 66:65–74. [PubMed: 17949989]

Bershadsky AD, Balaban NQ, Geiger B. Adhesion-dependent cell mechanosensitivity. Annual review of cell and developmental biology. 2003; 19:677–695.

Cancer Genome Atlas N. Comprehensive molecular portraits of human breast tumours. Nature. 2012; 490:61–70. [PubMed: 23000897]

Chambers SM, Shaw CA, Gatza C, Fisk CJ, Donehower LA, Goodell MA. Aging hematopoietic stem cells decline in function and exhibit epigenetic dysregulation. PLoS Biol. 2007; 5:e201. [PubMed: 17676974]

Chandler EM, Seo BR, Califano JP, Andresen Eguiluz RC, Lee JS, Yoon CJ, Tims DT, Wang JX, Cheng L, Mohanan S, et al. Implanted adipose progenitor cells as physicochemical regulators of breast cancer. Proc Natl Acad Sci U S A. 2012; 109:9786–9791. [PubMed: 22665775]

Charruyer A, Barland CO, Yue L, Wessendorf HB, Lu Y, Lawrence HJ, Mancianti ML, Ghadially R. Transit-amplifying cell frequency and cell cycle kinetics are altered in aged epidermis. The Journal of investigative dermatology. 2009; 129:2574–2583. [PubMed: 19458632]

Cho RH, Sieburg HB, Muller-Sieburg CE. A new mechanism for the aging of hematopoietic stem cells: aging changes the clonal composition of the stem cell compartment but not individual stem cells. Blood. 2008; 111:5553–5561. [PubMed: 18413859]

Choudhury S, Almendro V, Merino VF, Wu Z, Maruyama R, Su Y, Martins FC, Fackler MJ, Bessarabova M, Kowalczyk A, et al. Molecular profiling of human mammary gland links breast cancer risk to a p27(+) cell population with progenitor characteristics. Cell Stem Cell. 2013; 13:117–130. [PubMed: 23770079]

Cockburn K, Biechele S, Garner J, Rossant J. The Hippo pathway member Nf2 is required for inner cell mass specification. Curr Biol. 2013; 23:1195–1201. [PubMed: 23791728]

Dupont S, Morsut L, Aragona M, Enzo E, Giulitti S, Cordenonsi M, Zanconato F, Le Digabel J, Forcato M, Bicciato S, et al. Role of YAP/TAZ in mechanotransduction. Nature. 2011; 474:179–183. [PubMed: 21654799]

Engler AJ, Sen S, Sweeney HL, Discher DE. Matrix elasticity directs stem cell lineage specification. Cell. 2006; 126:677–689. [PubMed: 16923388]

Evans DG, Maher ER, Baser ME. Age related shift in the mutation spectra of germline and somatic NF2 mutations: hypothetical role of DNA repair mechanisms. Journal of medical genetics. 2005; 42:630–632. [PubMed: 16061561]

Garbe JC, Bhattacharya S, Merchant B, Bassett E, Swisshelm K, Feiler HS, Wyrobek AJ, Stampfer MR. Molecular distinctions between stasis and telomere attrition senescence barriers shown by long-term culture of normal human mammary epithelial cells. Cancer Res. 2009; 69:7557–7568. [PubMed: 19773443]

Garbe JC, Pepin F, Pelissier FA, Sputova K, Fridriksdottir AJ, Guo DE, Villadsen R, Park M, Petersen OW, Borowsky AD, et al. Accumulation of multipotent progenitors with a basal differentiation bias during aging of human mammary epithelia. Cancer Res. 2012; 72:3687–3701. [PubMed: 22552289]

Gudjonsson T, Ronnov-Jessen L, Villadsen R, Rank F, Bissell MJ, Petersen OW. Normal and tumor-derived myoepithelial cells differ in their ability to interact with luminal breast epithelial cells for polarity and basement membrane deposition. J Cell Sci. 2002; 115:39–50. [PubMed: 11801722]

Halder G, Dupont S, Piccolo S. Transduction of mechanical and cytoskeletal cues by YAP and TAZ. Nature reviews Molecular cell biology. 2012; 13:591–600.

Haralick RM, Shanmuga K, Dinstein I. Textural Features for Image Classification. Ieee T Syst Man Cyb *Smc3*. 1973:610–621.

Henry CJ, Marusyk A, DeGregori J. Aging-associated changes in hematopoiesis and leukemogenesis: what's the connection? Aging. 2011; 3:643–656. [PubMed: 21765201]

Hu M, Yao J, Carroll DK, Weremowicz S, Chen H, Carrasco D, Richardson A, Violette S, Nikolskaya T, Nikolsky Y, et al. Regulation of in situ to invasive breast carcinoma transition. Cancer Cell. 2008; 13:394–406. [PubMed: 18455123]

Imajo M, Miyatake K, Iimura A, Miyamoto A, Nishida E. A molecular mechanism that links Hippo signalling to the inhibition of Wnt/beta-catenin signalling. EMBO J. 2012; 31:1109–1122. [PubMed: 22234184]

Ishizaki T, Naito M, Fujisawa K, Maekawa M, Watanabe N, Saito Y, Narumiya S. p160ROCK, a Rho-associated coiled-coil forming protein kinase, works downstream of Rho and induces focal adhesions. FEBS letters. 1997; 404:118–124. [PubMed: 9119047]

Iwasa H, Maimaiti S, Kuroyanagi H, Kawano S, Inami K, Timalsina S, Ikeda M, Nakagawa K, Hata Y. Yes-associated protein homolog, YAP-1, is involved in the thermotolerance and aging in the nematode Caenorhabditis elegans. Exp Cell Res. 2013; 319:931–945. [PubMed: 23396260]

Kanai F, Marignani PA, Sarbassova D, Yagi R, Hall RA, Donowitz M, Hisaminato A, Fujiwara T, Ito Y, Cantley LC, et al. TAZ: a novel transcriptional co-activator regulated by interactions with 14-3-3 and PDZ domain proteins. The EMBO journal. 2000; 19:6778–6791. [PubMed: 11118213]

Kawamura K, Cheng Y, Suzuki N, Deguchi M, Sato Y, Takae S, Ho CH, Kawamura N, Tamura M, Hashimoto S, et al. Hippo signaling disruption and Akt stimulation of ovarian follicles for infertility treatment. Proc Natl Acad Sci U S A. 2013; 110:17474–17479. [PubMed: 24082083]

Kimura K, Ito M, Amano M, Chihara K, Fukata Y, Nakafuku M, Yamamori B, Feng J, Nakano T, Okawa K, et al. Regulation of myosin phosphatase by Rho and Rho-associated kinase (Rho-kinase). Science. 1996; 273:245–248. [PubMed: 8662509]

Knoth R, Singec I, Ditter M, Pantazis G, Capetian P, Meyer RP, Horvat V, Volk B, Kempermann G. Murine features of neurogenesis in the human hippocampus across the lifespan from 0 to 100 years. PLoS One. 2010; 5:e8809. [PubMed: 20126454]

Kuranda K, Vargaftig J, de la Rochere P, Dosquet C, Charron D, Bardin F, Tonnelle C, Bonnet D, Goodhardt M. Age-related changes in human hematopoietic stem/progenitor cells. Aging Cell. 2011; 10:542–546. [PubMed: 21418508]

Labarge MA, Garbe JC, Stampfer MR. Processing of human reduction mammoplasty and mastectomy tissues for cell culture. Journal of visualized experiments : JoVE. 2013

LaBarge MA, Nelson CM, Villadsen R, Fridriksdottir A, Ruth JR, Stampfer M, Petersen OW, Bissell MJ. Human mammary progenitor cell fate decsions are products of interactions with combinatorial microenvironments. Integrative Biology. 2009; 1:70–79. [PubMed: 20023793]

Lim E, Vaillant F, Wu D, Forrest NC, Pal B, Hart AH, Asselin-Labat ML, Gyorki DE, Ward T, Partanen A, et al. Aberrant luminal progenitors as the candidate target population for basal tumor development in BRCA1 mutation carriers. Nat Med. 2009; 15:907–913. [PubMed: 19648928]

Lui C, Lee K, Nelson CM. Matrix compliance and RhoA direct the differentiation of mammary progenitor cells. Biomechanics and modeling in mechanobiology. 2011

Moerman EJ, Teng K, Lipschitz DA, Lecka-Czernik B. Aging activates adipogenic and suppresses osteogenic programs in mesenchymal marrow stroma/stem cells: the role of PPAR-gamma2 transcription factor and TGF-beta/BMP signaling pathways. Aging Cell. 2004; 3:379–389. [PubMed: 15569355]

Nguyen LV, Makarem M, Carles A, Moksa M, Kannan N, Pandoh P, Eirew P, Osako T, Kardel M, Cheung AM, et al. Clonal Analysis via Barcoding Reveals Diverse Growth and Differentiation of Transplanted Mouse and Human Mammary Stem Cells. Cell Stem Cell. 2014; 14:253–263. [PubMed: 24440600]

Pang WW, Price EA, Sahoo D, Beerman I, Maloney WJ, Rossi DJ, Schrier SL, Weissman IL. Human bone marrow hematopoietic stem cells are increased in frequency and myeloid-biased with age. Proc Natl Acad Sci U S A. 2011; 108:20012–20017. [PubMed: 22123971]

Pantic I, Pantic S, Basta-Jovanovic G. Gray level co-occurrence matrix texture analysis of germinal center light zone lymphocyte nuclei: physiology viewpoint with focus on apoptosis. Microscopy and microanalysis : the official journal of Microscopy Society of America, Microbeam Analysis Society, Microscopical Society of Canada. 2012; 18:470–475.

Paszek MJ, Zahir N, Johnson KR, Lakins JN, Rozenberg GI, Gefen A, Reinhart-King CA, Margulies SS, Dembo M, Boettiger D, et al. Tensional homeostasis and the malignant phenotype. Cancer Cell. 2005; 8:241–254. [PubMed: 16169468]

Provenzano PP, Inman DR, Eliceiri KW, Keely PJ. Matrix density-induced mechanoregulation of breast cell phenotype, signaling and gene expression through a FAK-ERK linkage. Oncogene. 2009; 28:4326–4343. [PubMed: 19826415]

Rios AC, Fu NY, Lindeman GJ, Visvader JE. In situ identification of bipotent stem cells in the mammary gland. Nature. 2014

Santagata S, Thakkar A, Ergonul A, Wang B, Woo T, Hu R, Harrell JC, McNamara G, Schwede M, Culhane AC, et al. Taxonomy of breast cancer based on normal cell phenotype predicts outcome. J Clin Invest. 2014; 124:859–870. [PubMed: 24463450]

Seidler HB, Utsuyama M, Nagaoka S, Takemura T, Kitagawa M, Hirokawa K. Expression level of Wnt signaling components possibly influences the biological behavior of colorectal cancer in different age groups. Experimental and molecular pathology. 2004; 76:224–233. [PubMed: 15126105]

Shehata M, Teschendorff A, Sharp G, Novcic N, Russell A, Avril S, Prater M, Eirew P, Caldas C, Watson CJ, et al. Phenotypic and functional characterization of the luminal cell hierarchy of the mammary gland. Breast Cancer Res. 2012; 14:R134. [PubMed: 23088371]

Stampfer, MM.; LaBarge, MA.; Garbe, JC. An Integrated Human Mammary Epithelial Cell Culture System for Studying Carcinogenesis and Aging. In: Schatten, H., editor. In Cell and Molecular Biology of Breast Cancer. New York: Springer; 2013. p. 323-361.

Stoll EA, Habibi BA, Mikheev AM, Lasiene J, Massey SC, Swanson KR, Rostomily RC, Horner PJ. Increased re-entry into cell cycle mitigates age-related neurogenic decline in the murine subventricular zone. Stem Cells. 2011; 29:2005–2017. [PubMed: 21948688]

Tamada M, Sheetz MP, Sawada Y. Activation of a signaling cascade by cytoskeleton stretch. Developmental cell. 2004; 7:709–718. [PubMed: 15525532]

Tse JR, Engler AJ. Preparation of hydrogel substrates with tunable mechanical properties. Current protocols in cell biology / editorial board, Juan S Bonifacino [et al] *Chapter*. 2010; 10:Unit 10–Unit 16.

Villadsen R, Fridriksdottir AJ, Ronnov-Jessen L, Gudjonsson T, Rank F, Labarge MA, Bissell MJ, Petersen OW. Evidence for a stem cell hierarchy in the adult human breast. J Cell Biol. 2007; 177:87–101. [PubMed: 17420292]

Vogel V, Sheetz M. Local force and geometry sensing regulate cell functions. Nat Rev Mol Cell Biol. 2006; 7:265–275. [PubMed: 16607289]

Wada K, Itoga K, Okano T, Yonemura S, Sasaki H. Hippo pathway regulation by cell morphology and stress fibers. Development. 2011; 138:3907–3914. [PubMed: 21831922]

Yu H, Mouw JK, Weaver VM. Forcing form and function: biomechanical regulation of tumor evolution. Trends in cell biology. 2011; 21:47–56. [PubMed: 20870407]

Zhao B, Li L, Lu Q, Wang LH, Liu CY, Lei Q, Guan KL. Angiomotin is a novel Hippo pathway component that inhibits YAP oncoprotein. Genes & development. 2011; 25:51–63. [PubMed: 21205866]

Zhao B, Wei X, Li W, Udan RS, Yang Q, Kim J, Xie J, Ikenoue T, Yu J, Li L, et al. Inactivation of YAP oncoprotein by the Hippo pathway is involved in cell contact inhibition and tissue growth control. Genes & development. 2007; 21:2747–2761. [PubMed: 17974916]

Highlights

- Mechano-response in multipotent human mammary progenitors is age-dependent
- The mechano-sensing apparatuses are equally active in young and old progenitors
- Hippo-pathway transducers YAP and TAZ exhibit age-dependent activation efficiencies
- YAP activation in progenitors causes age-dependent differentiation patterns

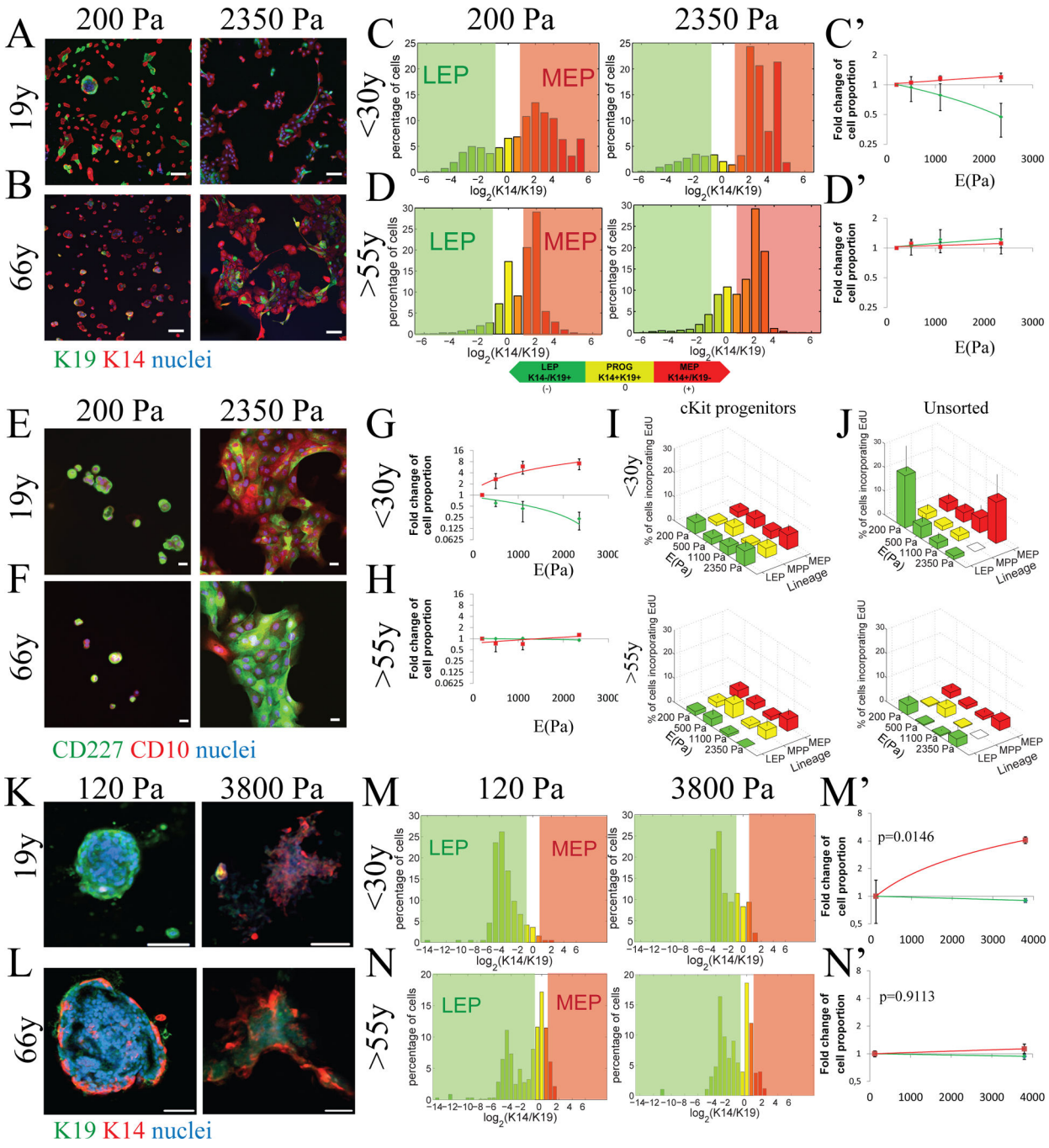

Figure 1. Aging alters differentiation patterns in response to substrate elastic modulus

Representative IF analysis of progenitors from young (240L, 19y) and (B) an older (122L, 66y) strains stained for K19 (green), K14 (red) and DAPI (blue) after 48h of culture on PA gels with increasing elastic modulus (E(Pa)). Bars represent 100μm. (C & D) Histograms represent $\log_2$-transformed ratios of K14 to K19 protein expression in single cells on 2D PA gels with increasing stiffness, histograms are heat mapped to indicate cells with the phenotypes of K14-/K19+ LEPs (green), K14+/K19+ progenitors (yellow), and K14+/K19- MEPs (red). Corresponding linear regression plots of LEP and MEP proportions as a

function of modulus are shown for (C) women <30y (LEP p=0.0429, r^2= 0.2086, MEP p=0.0475, r^2= 0.2009 n=5) and (D') women >55 (LEP p=0.4812, r^2= 0.0296, MEP p=0.5138, r^2= 0.0240, n=5). Regressions are fold change of lineage proportions compared to cKit+ on 200Pa condition ± s.e.m. (E) Representative IF analysis of progenitors from young (240L, 19y) and (F) an older (122L, 66y) strains stained for CD227 (green), CD10 (red) and DAPI (blue) after 48h of culture on PA gels with increasing elastic modulus. Bars represent 20μm. (G) Linear regression of fold change of LEP (CD227+/CD10-) and MEP (CD227-/CD10+) proportions as function of elastic modulus in women <30y (LEP p=0.0080, r^2= 0.5219, MEP p=0.0198, r^2= 0.4340 n=3) and (H) women >55y (LEP p=0.4689, r^2= 0.0536, MEP p=0.1937, r^2= 0.5219, n=3). Linear regressions are of fold change of lineage proportions normal to 200Pa condition ± s.e.m. Percentage of cells incorporating EdU as function of lineages and stiffness in (I) cKit+ HMEC and (J) unsorted HMEC (MEP from women <30y linear regression p=0.0270, r^2=0.9467, LEP from women <30y t-test 200Pa vs 2350Pa p=0.0153, n=5). Data are means ± s.e.m. (K and L) Representative immunofluorescence of K19 (green), K14 (red) and DAPI (blue) of passage 1 cKit+ HMEC from a 19y and a 65y woman after 7 days of culture encapsulated in 3D hyaluronic acid (HA) gels. Bars represent 20nm. (M and N) Histograms represent $\log_2$-transformed ratios of K14 to K19 protein expression in single cells in 3D HA gels, histograms are heat mapped to indicate cells with the phenotypes of K14-/K19+ LEPs (green), K14+/K19+ progenitors (yellow), and K14+/K19- MEPs (red). (M' and N') Fold changes of lineage proportions normal to 120Pa condition (Chi-squared test women <30y p=0.0146, women >55y p=0.9113). See also Figure S2, S3, S4 and Table S2.

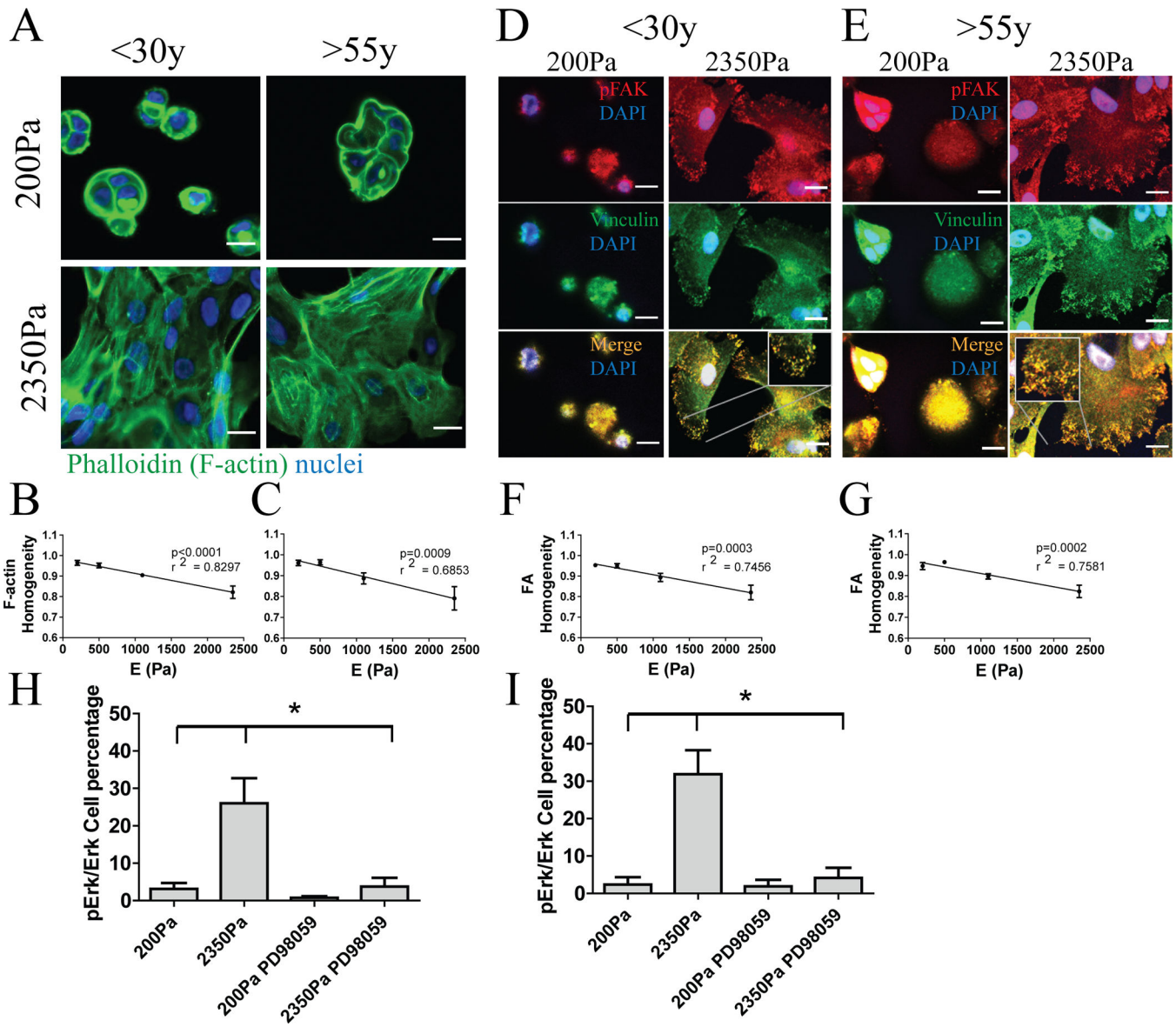

Figure 2. Mechano-sensing apparatuses function independently of age to generate actin stress fibers, focal adhesions, and ERK activation

(A) Representative immunofluorescence of F-actin (green) in cKit+ HMEC from a young strain (240L, 19y) and an older strain (122L, 66y) on PA gels of increasing stiffness. (B and C) Image quantification of F-actin homogeneity using feature detection (B, $p<0.0001$ and $r^2=0.8297$, slope= −6,805e-5 ± 9,749e-6, n=3; C, $p<0.001$ and $r^2=0.6853$, slope=-8,454e-5 ± 1,811e-5, n=3). The slopes are not significantly different (p=0.5699). Representative immunofluorescence images of pFAK (red) and vinculin (green), which overlapped (yellow), from confocal microscopy are shown in cKit+ HMEC from (D) a young strain (240L 19y) and (E) an older strain (122L 66y). Cells are shown at the substrata interface. Bars represent 20μm. (F and G) Image quantification of vinculin and pFAK homogeneity (F, $p<0.001$ and $r^2=0.7456$, slope=-6,512e-5 ± 1,203e-5, n=3; G, $p<0.001$ and $r^2=0.7581$, slope=-6,356e-5 ± 1,136e-5, n=3). The slopes are not significantly different (p=0.8124).

Data are means ± s.e.m. (H and I) Ratio of pERK positive to ERK positive cell number in cKit+ HMEC from <30y (n=3) and >55y (n=3) strains on 200Pa and 2350Pa.

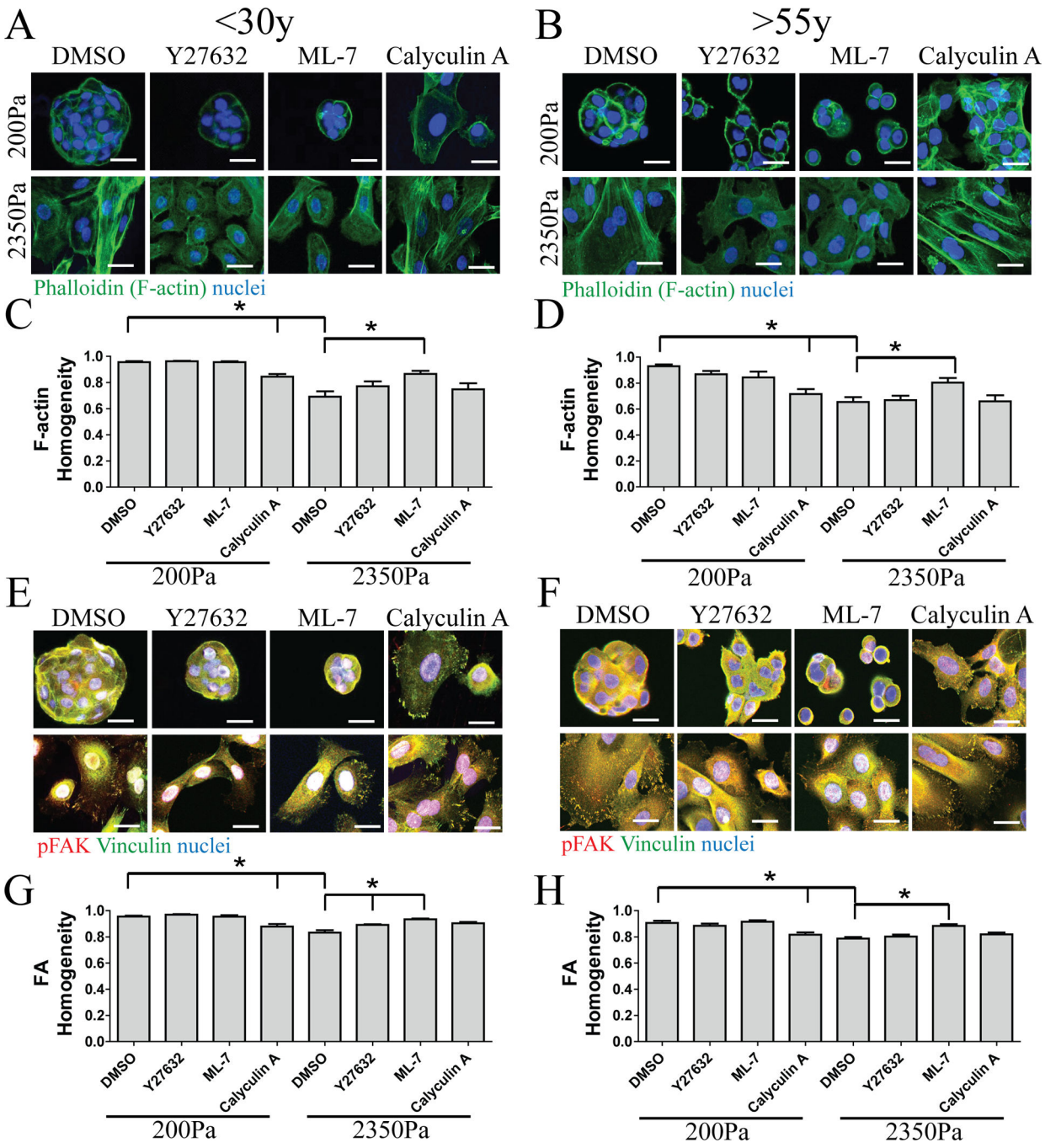

Figure 3. Perturbations of actinomyosin regulators elicit parallel mechano-sensing phenotypes in progenitors from young and old age groups

(A and B) Representative immunofluorescence of F-actin with phalloidin (green) in cKit+ HMEC from (A) a young strain (240L, 19y) and (B) an older strain (122L, 66y). Image quantification of F-actin homogeneity in (C) younger cKit+ (n=3) and (D) older cKit+ (n=3). Merged images of immunofluorescence of pFAK (red) and vinculin (green), overlap is (yellow), in cKit+ HMEC from (E) the young strain and (F) the older strain. Bars represent 20μm. Image quantification of vinculin and pFAK homogeneity in (G) young cKit + (n=3) and (H) older cKit (n=3). See also figure S5.

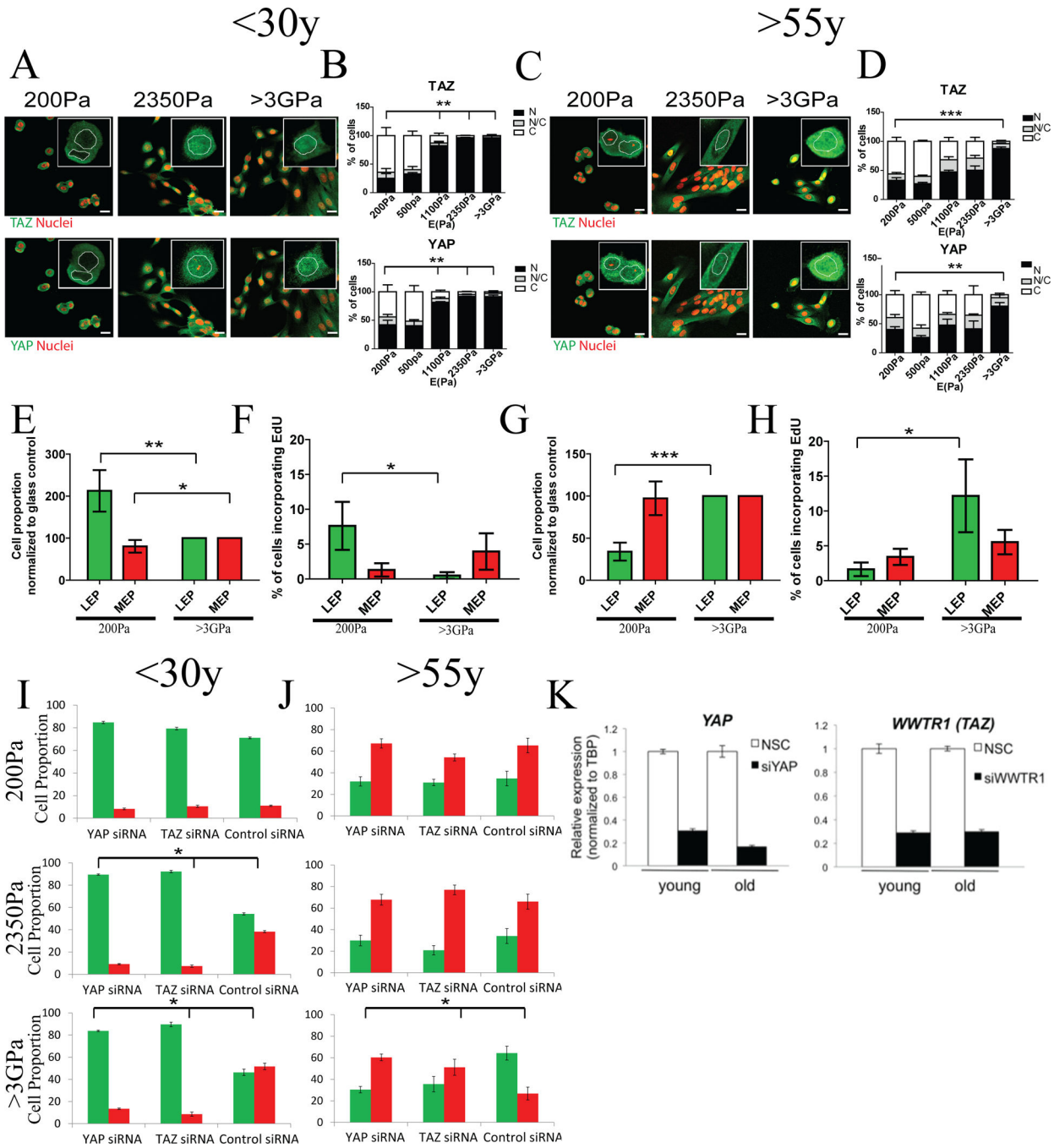

Figure 4. YAP and TAZ activation are altered during aging

Representative immunofluorescence of TAZ (red), YAP (green), and DAPI (blue) in cKit+ HMEC from (A) a young strain (240L, 19y) and (C) an older strain (353P, 72y). Bars represent 20μm. Bar plots represent the distribution of YAP and TAZ (N: predominantly in the nucleus, N/C: equally distributed, C: predominantly in the cytoplasm) from over 100 cells/strain in (B) younger (n=3) and (D) older (n=3) strains. K19+LEP and K14+MEP proportions derived from cKit+ HMEC from (E) younger (n=5) and (G) older (n=5) women. Data are fold change of cell proportions compared to glass control ± s.e.m. Percentage of

EdU^{+} LEP and MEP derived from cKit+ HMEC from (F) younger (n=5) and (H) older (n=5) women. Data are means ± s.e.m. K19+LEP and K14+MEP proportions derived from cKit+ HMEC from (I) younger and (J) older strains transfected with YAP or TAZ siRNA. (K) Bar graphs of YAP and TAZ transcript knockdown following siRNA treatment, NSC scrambled control siRNA.

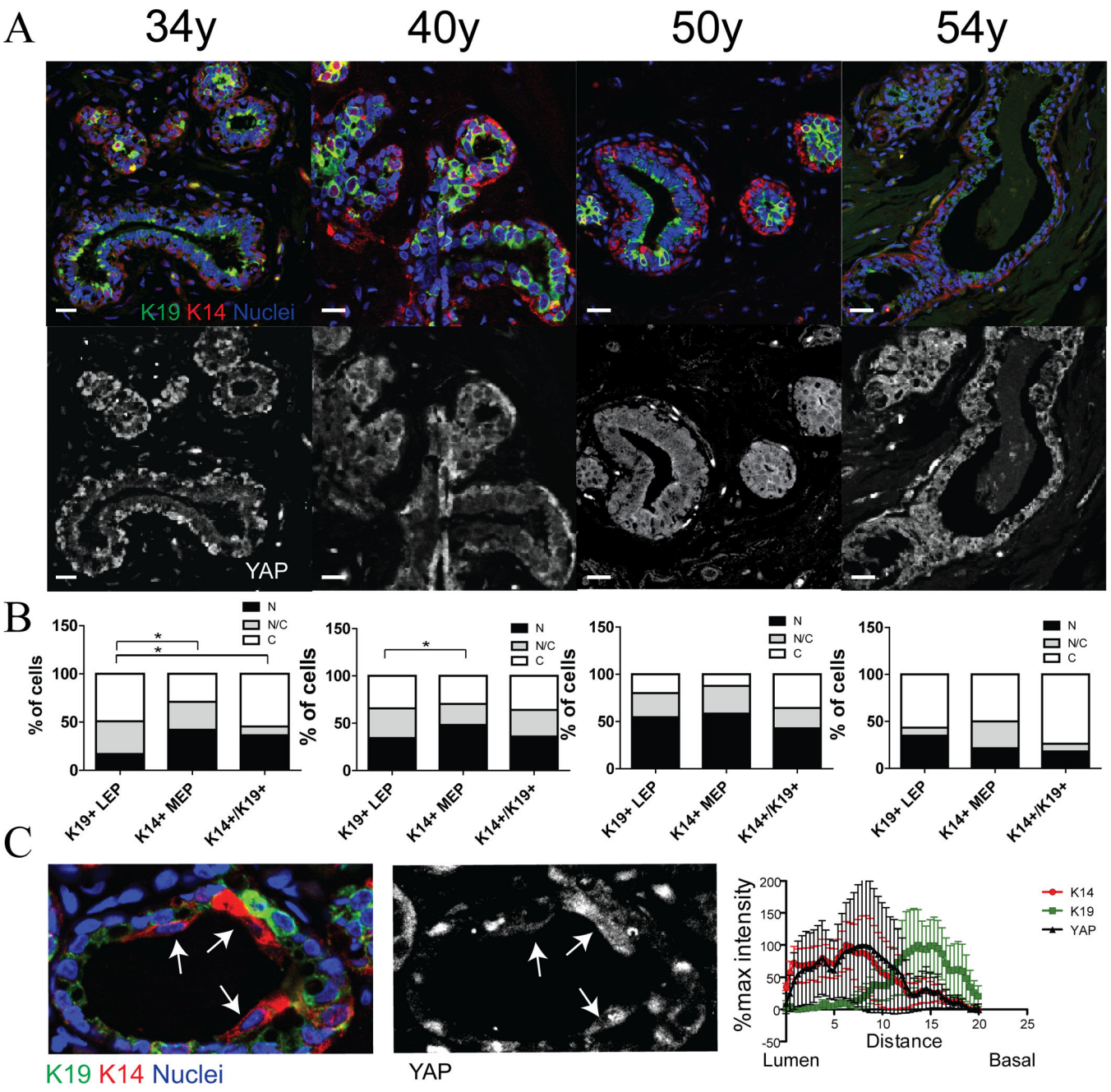

Figure 5. YAP localization changes with age *in vivo*

(A) Representative immunofluorescence of K14 (red), K19 (green), YAP (white) and DAPI (blue) in human mammary breast sections from four women (aged 34y, 40y, 50y, 54y). Bars represent 20μm. (B) Bar plots represent the distribution of YAP (N: predominantly in the nucleus, N/C: equally distributed, C: predominantly in the cytoplasm) from over 100 cells/ woman. (C) YAP signal isolation from the immunofluorescence of K14 (red), K19 (green), YAP (white) and DAPI (blue) from the 34y woman. Arrows identify luminal-positioned $K14^{+}/K19^{low/-}$ cells. The line graph shows mean pixel intensities from the lumen to the

basal side of the structure in 10 different examples of K14+ luminal cells. See also Figure S6.

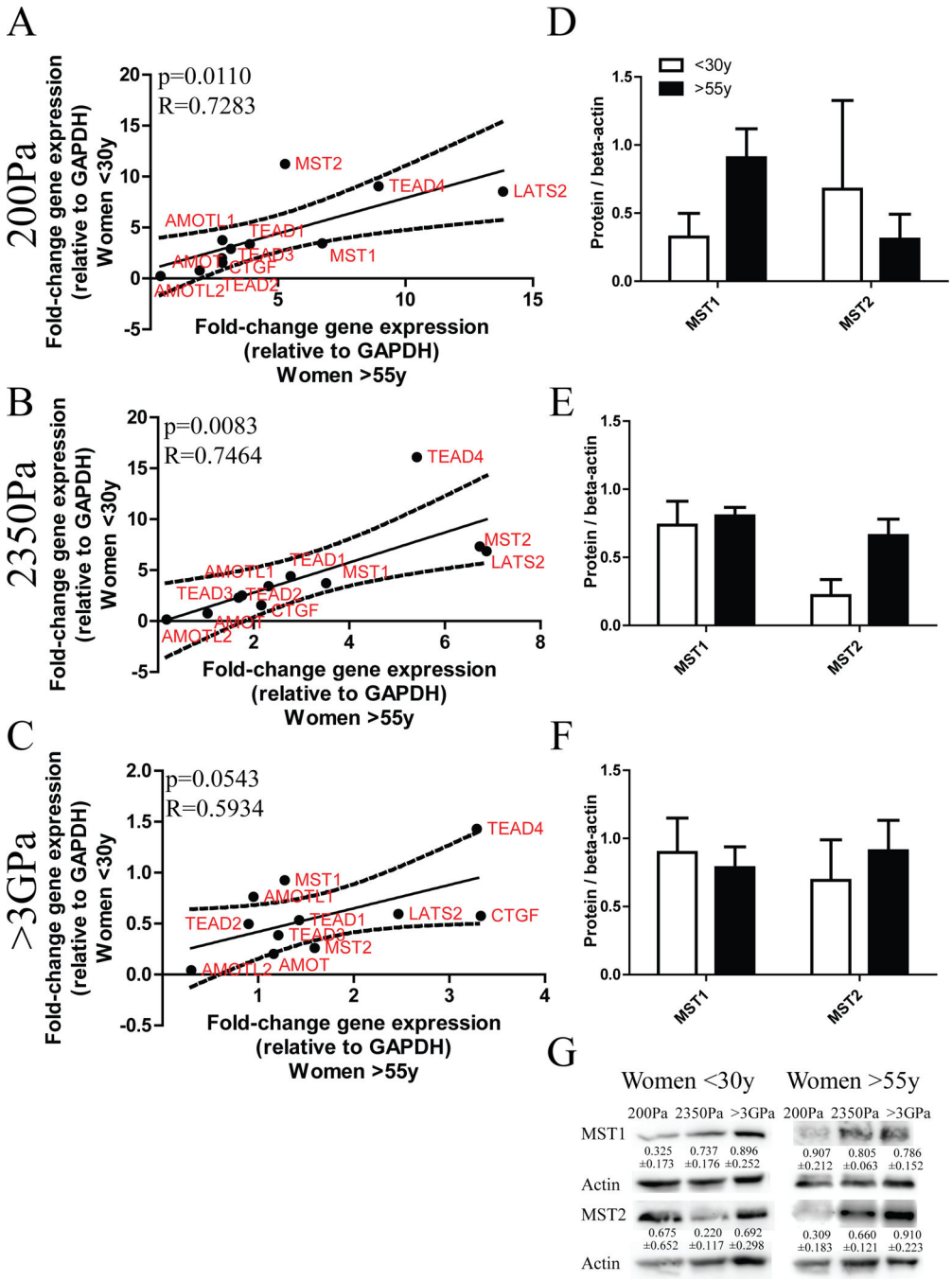

Figure 6. Age-dependent patterns of Hippo pathway components

Correlation of gene expression between cKit+ HMEC from younger (n=3) and older (n=3) strains after 24h on (A) 200Pa (p=0.0110, R=0.7283) (B) 2350Pa PA gels (p=0.0083, R=0.7464) and (C) >3GPa substrate (p=0.0543, R=0.5934). Data are normalized to GAPDH expression. Western blot densitometric analysis of MST1 and MST2 from cKit+ HMEC from younger (n=3) and older (n=3) strains after 24h on (D) 200Pa, (E) 2350Pa PA gels and (F) >3GPa substrate. Data are normalized to beta-actin protein content and are mean ± s.e.m.

(G) Representative western blot with quantification from a young (240L, 19y) and an older strain (122L, 66y).

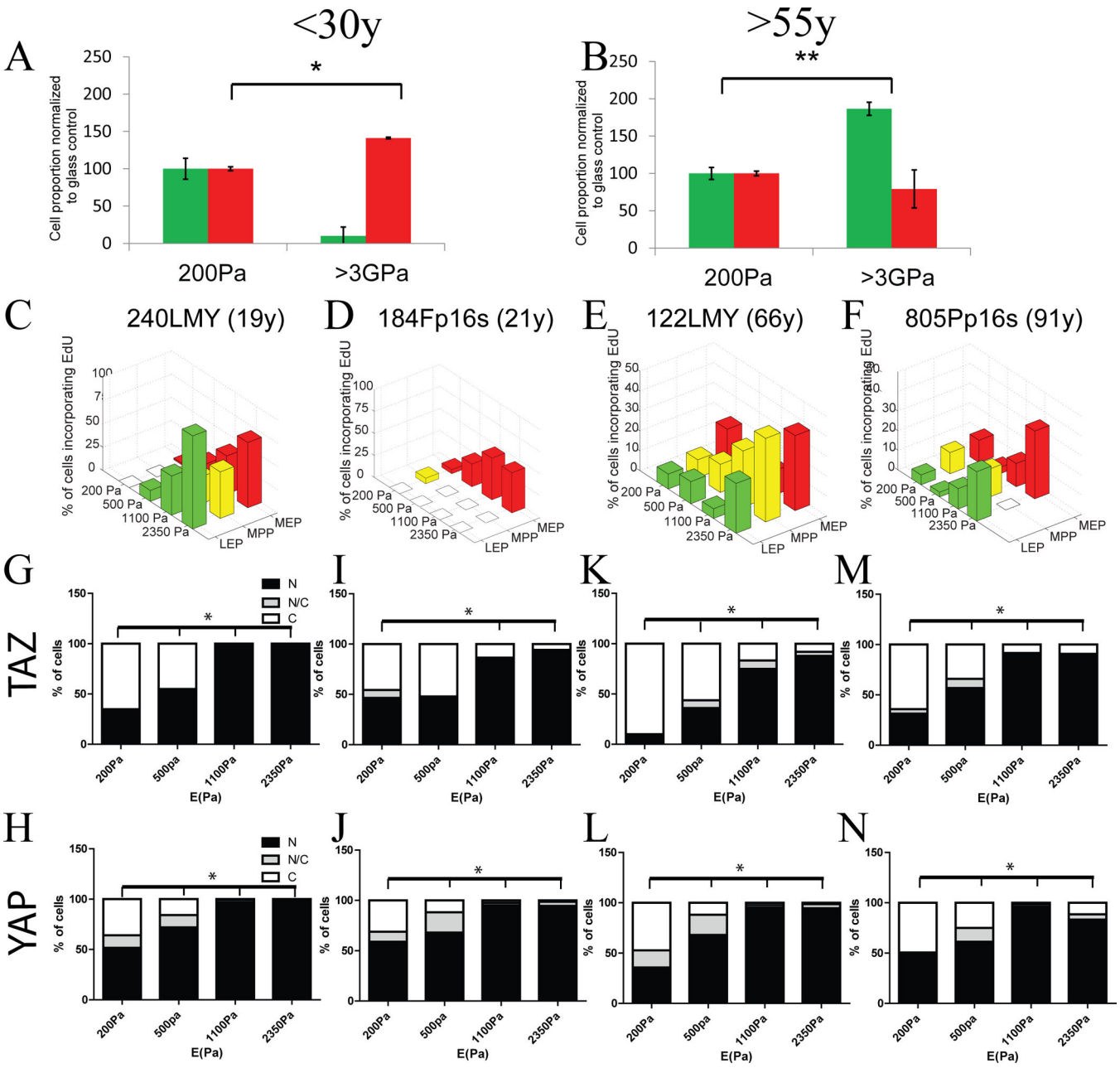

Figure 7. Immortalization restores responsiveness to physiological stiffness in older HMEC

K19+LEP and K14+MEP proportions derived from immortalized cell lines from (A) younger (p=0.0111, n=2 individuals in triplicate) and (B) older (p=0.0056, n=2 individuals in triplicate) women. Data are fold change of cell proportions compared to glass control ± s.e.m. (C–F) Percentage of cells from immortalized cell lines derived from primary strains (240LMY at passage 25, 184Fp16s at passage 31, 122LMY at passage 19 and 805Pp16s at passage 29) incorporating EdU as a function of lineage, as defined by K14 and K19 expression, and stiffness. (G–N) Bar plots represent the distribution of YAP and TAZ (N: predominantly in the nucleus, N/C: equally distributed, C: predominantly in the cytoplasm) from over 100 cells/lineage in immortalized cell lines. By comparison to the other cell lines,

184F derivatives are known to be mainly basal at the expense of LEP and progenitor See also Figure S7.